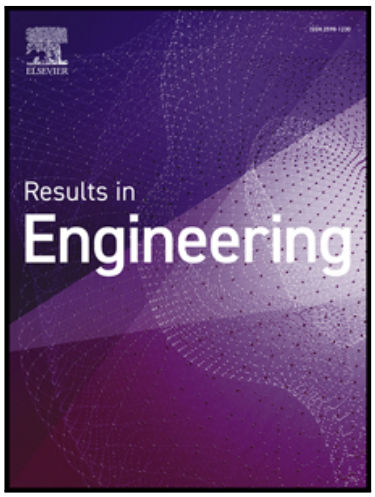

Automated Design of Additively Manufactured Reactors for Decentralized CO2-to-Methanol Production

Mertcan Kaya, Christoph Klahn

PII: S2590-1230(26)04036-3
DOI: https://doi.org/10.1016/j.rineng.2026.113025
Reference: RINENG 113025

To appear in: *Results in Engineering*

Received date: 15 April 2026
Revised date: 8 September 2026
Accepted date: 15 September 2026

Please cite this article as: Mertcan Kaya, Christoph Klahn, Automated Design of Additively Manufactured Reactors for Decentralized CO2-to-Methanol Production, *Results in Engineering* (2025), doi: https://doi.org/10.1016/j.rineng.2026.113025

Highlights

of the Article

Automated Design of Additively Manufactured Reactors for Decentralized CO2-to-Methanol Production

- Automated generation of 3D-printable methanol reactors from a target production rate
- Continuous workflow from user requirements to print-ready reactor geometry
- Combined geometry and process optimization from lab (0.125 L/day) to container scale (50 L/day)
- Design time of 105 min at lab scale and 27 h at container scale
- Experimental lab-scale validation of the proposed design automation tool

Automated Design of Additively Manufactured Reactors for Decentralized CO_2-to-Methanol Production

Mertcan Kaya[a,*], Christoph Klahn[a,b]

[a]*Karlsruhe Institute of Technology (KIT), Institute for Micro Process Engineering (IMVT), 76344 Eggenstein-Leopoldshafen, Germany*
[b]*Karlsruhe Institute of Technology (KIT), Institute of Mechanical Process Engineering and Mechanics (MVM), 76131 Karlsruhe, Germany*

Abstract

The transition to decentralized energy systems increases the demand for adaptable and scalable reactors. Power-to-Methanol (PtM) converts renewable electricity, green H_2, and captured CO_2 into a liquid energy carrier. The reaction is exothermic, so reactor design governs both the achievable methanol production rate and the thermal control of the system. Additive manufacturing (AM) widens the accessible design space, but the development of complex reactor geometries depends on computer-aided design (CAD) expertise that is not common among chemical engineers. To address this limitation, this study presents a design automation tool for the development of customized reactors across varying operational conditions and production scales. The tool integrates automated geometry generation, simulation-based performance evaluation, and AM design constraints within a single workflow. Based on a defined target methanol production rate, it generates manufacturing-ready reactor geometries without manual CAD input. The total design time is approximately 105 minutes for a lab-scale reactor at 0.125 L/day and 27 hours for a container-scale reactor at 50 L/day. The underlying computational fluid dynamics (CFD) model is validated against lab-scale experiments on additively manufactured reactor configurations at varying inlet flow rates. Simulated and measured outlet flows agree with a root mean square error (RMSE) of 4.11, 3.67 and 34.15 mL_s/min for CO, CO_2 and H_2. This work connects the design stage to the manufactured reactor, supporting the deployment of PtM technologies in decentralized energy systems.

Keywords: Design Automation, Chemical Engineering, Additive Manufacturing, Reaction Engineering, Energy Storage

1. Introduction

The growing global population and associated CO_2 emissions are intensifying the threat of climate change. In response, innovative technologies have emerged to reduce CO_2 emissions and enhance renewable energy storage, with several already reaching industrial application

*Corresponding author
Email address: mertcan.kaya@kit.edu (Mertcan Kaya)

[1–4]. One notable advancement is the Power-to-Methanol (PtM) technology, which utilizes renewable energy sources such as wind and solar to produce green methanol through hydrogen electrolysis and CO_2 capture [5, 6]. Green methanol serves as a sustainable fuel alternative, particularly in the shipping industry, offering a viable pathway to decarbonize maritime transport [6, 7]. Within the PtM chain, the present work addresses the methanol synthesis step, in which the captured CO_2 is hydrogenated to methanol. This reaction is exothermic and necessitates precise temperature control to prevent side reactions and catalyst deactivation. Optimizing heat and mass transfer through advanced fluid dynamics is crucial to enhance methanol production rate, underscoring the significance of reactor design in methanol synthesis [8, 9]. However, achieving optimal reactor performance is not only a technical challenge but also highly dependent on the scale and the system's inherent operational constraints.

Traditionally, methanol production has relied on large-scale, centralized facilities. However, the shift toward decentralized systems is gaining importance due to evolving energy conversion strategies. While decentralization offers advantages such as increased flexibility and local energy integration, it also introduces challenges related to geographical conditions, including variations in renewable energy availability and differing safety regulations [10]. These factors necessitate reactor designs tailored to specific regional constraints, highlighting the need for mass customization. This shift opens new avenues for microreactors and sophisticated reactor designs enabled by additive manufacturing (AM). Microreactors offer enhanced control over reaction parameters, leading to improved efficiency and safety. AM facilitates the creation of complex reactor geometries tailored to specific process requirements [11–13], offering new possibilities for methanol synthesis in decentralized settings. Despite the advantages offered by AM reactor designs, they introduce new challenges. The creation of intricate reactor geometries requires expertise in computer-aided design (CAD), a skillset that is not commonly found among chemists and chemical engineers [14, 15]. This skill gap presents a significant barrier to the widespread adoption of AM reactors in methanol synthesis and other catalytic applications. Moreover, manual reactor design and its optimization for manufacturability are time-consuming, even though commercial reactor design features are typically highly standardized and offer little to no additional functional benefits.

To address this challenge, technologies for design automation in reactor development are increasingly needed. Bridging this gap would empower chemical engineers to create custom reactors tailored to their specific methanol synthesis requirements. To realize this vision, this paper introduces a reactor design automation tool developed to automate the design and optimization of methanol synthesis reactors. In contrast to existing reactor design automation approaches, which address individual stages of the design process, the tool couples process-level reactor sizing, algorithmic geometry generation, multiphysics evaluation, and AM manufacturability constraints within a single workflow that leads from a user-defined target methanol production rate to a print-ready reactor geometry. Targeted specifically at decentralized PtM applications, it covers the scale range from lab to container-scale reactors. The tool is furthermore structured to be extendable toward increasingly complex reactor designs in the future. The key contributions of this paper are as follows:

- Development of a fully automated design tool that translates a user-defined production target into print-ready reactor designs, with AM design rules enforced during geometry

generation

- Significant reduction in reactor development time, enabling the transition from design to fabrication within hours
- Development of a tool for mass customization of reactor designs, allowing adaptation to various operational conditions and renewable energy sources in decentralized systems
- Experimental validation of the proposed tool, demonstrating its practical applicability and effectiveness in optimizing reactor performance for achieving the target methanol production rate

This paper is structured as follows: Section 2 provides a comprehensive review of the state of the art in methanol synthesis reactor design and development, highlighting the need for an automated tool to streamline reactor engineering. Section 3 introduces the proposed automated design tool for methanol synthesis reactors, detailing its workflow and capabilities. Section 4 presents the experimental validation of the tool, ensuring the reliability of the simulations used in the design process. Section 5 discusses the results, evaluating the tool's effectiveness and demonstrating its practical applicability.

2. State of the Art

2.1. Methanol Synthesis and Reactor Concepts

Methanol synthesis involves the hydrogenation of carbon dioxide (CO_2), reverse water-gas shift (RWGS) reaction and the hydrogenation of carbon monoxide (CO) under elevated pressures (50–100 bar) and moderate temperatures (200–300°C) using Cu/Zn-based catalysts [16]. The relevant reactions in methanol synthesis are defined as follows:

$$CO + 2H_2 \rightleftharpoons CH_3OH \quad \Delta H = -90.64\,\mathrm{kJ/mol} \tag{1}$$

$$CO_2 + 3H_2 \rightleftharpoons CH_3OH + H_2O \quad \Delta H = -49.67\,\mathrm{kJ/mol} \tag{2}$$

$$CO_2 + H_2 \rightleftharpoons CO + H_2O \quad \Delta H = 41\,\mathrm{kJ/mol} \tag{3}$$

Recent kinetic studies and experimental data indicate that methanol formation predominantly occurs through CO_2 hydrogenation [5, 17], which is also the pathway of interest for reducing CO_2 emissions through the utilization of renewable energy sources. This study therefore focuses on reaching a user-defined target methanol production rate by accelerating CO_2 hydrogenation. As shown in Equations 1 and 2, the reaction is exothermic and requires an efficient cooling system to regulate the temperature in the reaction zone and prevent catalyst deactivation due to excessive heat. Accordingly, industrial reactor concepts are mainly distinguished by their heat-removal strategy and their ability to maintain near-isothermal operation (see Figure 1). Heat is either removed through catalyst-filled tubes cooled by boiling water, as in the Lurgi tubular reactor, through hollow cooling plates embedded in the catalyst bed, as in the Methanol Casale IMC reactor, through internal heat exchange, as in the Linde Variobar and the Mitsubishi Superconverter, or through a liquid phase, as in the Air Products LPMEOH reactor [5, 18–20].

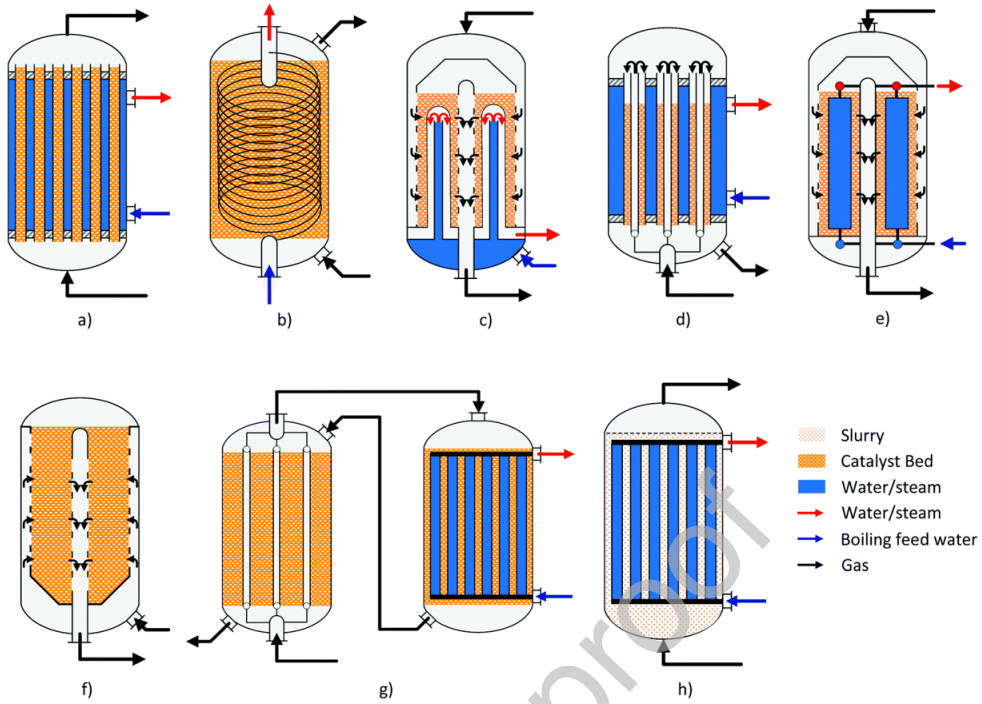

Figure 1: Simplified schematic representations of established industrial methanol synthesis reactors, illustrating the range of heat-removal strategies that motivate the AM-based reactor concept adopted in this work: (a) the Lurgi tubular reactor, (b) the Linde Variobar system, (c) the Toyo MRF reactor, (d) the Mitsubishi Superconverter, (e) the Methanol Casale IMC reactor, (f) the Haldor Topsøe adiabatic reactor, (g) the Lurgi MegaMethanol process, and (h) the Air Products LPMEOH reactor [5]

While large-scale industrial reactors dominate commercial methanol production, microreactors offer significant advantages in temperature control and reaction efficiency, despite their limited adoption in the industry. Bakhtiary-Davijany et al. maintained an isothermal temperature profile in a single-slit micro packed bed reactor using thermal oil [21], and Arab et al. transferred the Lurgi tubular principle to a multitubular configuration with a monolithic catalytic insert, improving heat transfer in the reaction zone through increased thermal conduction [22]. AM reactors build on these developments by combining the advantages of microreactors with the adaptability required for decentralized systems. Li et al. designed and manufactured an AM reactor for methanol synthesis and assessed its performance through computational fluid dynamics (CFD) simulations [23], while further concepts have been demonstrated for methanol synthesis [24], Fischer-Tropsch synthesis [25] and methanation [12], confirming the potential of AM for chemical reactor development. However, in all of these cases the reactor geometries are developed manually, without an automated design process, and structural safety verification is not integrated into the design loop. Furthermore, none of these approaches provides a continuous workflow from a defined production target to a print-ready CAD model, and the scaling of such reactors toward industrial production volumes remains largely unaddressed.

2.2. Design for Powder Bed Fusion Using Laser Beam for Metals (PBF-LB/M)

AM encompasses various techniques, but PBF-LB/M has emerged as a leading technology for high-performance reactors, enabling the fabrication of complex geometries with integrated cooling channels and stiffening structures to ensure mechanical strength under high pressure and high temperature operational conditions. Owing to its ability to produce parts with material properties comparable to those of commercial metals, PBF-LB/M offers significant advantages in reactor development.

The PBF-LB/M process relies on the layer-by-layer selective melting of metal powder using a laser, following a CAD-defined cross-section, with each layer solidifying before the next is applied. To maintain dimensional accuracy, overhanging structures exceeding 45° typically require support, yet excessive reliance on supports increases post-processing time and may be impractical for internal geometries. Therefore, minimizing support structures through design optimization is essential to enhance manufacturability and reduce material waste. Additionally, internal features such as cooling channels must incorporate accessible entry points to ensure complete powder removal. The design constraints of PBF-LB/M are influenced by factors including material properties, process parameters, and machine specifications, necessitating a comprehensive understanding of Design for Additive Manufacturing (DfAM) principles. [26–29]

Table 1: Applied PBF-LB/M design rules and their treatment within the design automation tool

Design rule	**Applied value**	**Treatment in the tool**
Minimum wall thickness	0.8 mm	Enforced as the lower bound of the FEA-based wall thickness optimization
Overhang angle	45°	Ensured by the algorithmic design of the reactor geometry
Powder removal	No enclosed cavities	Ensured by the algorithmic design of the reactor geometry
Build volume	$120 \times 120 \times 200$ mm^3 (lab) $350 \times 350 \times 500$ mm^3 (container)	User input, checked against the generated geometry

In this study, stainless steel 316L is selected as the printing material, as its mechanical properties are sufficient for the considered operating conditions and it is well established for PBF-LB/M, although other materials can be used if the operating conditions require it. The reactor design is developed in accordance with established design guidelines reported in multiple sources [26–28] to optimize manufacturability and performance in methanol synthesis applications. The applied design rules and their treatment within the design automation tool are summarized in Table 1. The overhang angle of 45° is taken from these guidelines, whereas

the minimum wall thickness of 0.8 mm is determined for the employed machine and the qualified standard parameter set for stainless steel 316L. As the complexity of AM-compatible geometries increases, however, applying these DfAM principles manually becomes increasingly demanding. Design automation addresses this by systematically enforcing the rules during geometry generation, enabling efficient exploration of manufacturable alternatives.

2.3. Design Automation in Process Engineering

Design automation is applied across various fields of mechanical engineering, including aerospace, industrial robots and multi-flow nozzles [30–34], with the primary objective of minimizing repetitive design tasks, which Stokes estimates to account for approximately 80% of manual design activity [35]. Two main approaches are established in the literature [36, 37]: Computational design synthesis (CDS), which automates the generation of design alternatives in the early design stages to systematically explore the design space [38], and knowledge based engineering (KBE), which formalizes and reuses domain-specific engineering knowledge to identify optimal solutions within that space [39].

Table 2: Comparison of the proposed design automation tool with existing automated reactor design approaches

	Hou et al. [14]	**Savage et al. [40]**	**This work**
Design basis	Predefined modules	Single geometry family	Algorithmic generation
Simulation	–	CFD	PFR, FEA, CFD
AM constraints	–	–	Integrated
Scale	Lab	Lab	Lab to container

Despite the limited application of design automation in process engineering, it provides significant advantages in addressing complex challenges such as temperature and flow control, pressure drop minimization, and mixing enhancement. Several studies have demonstrated the effectiveness of automated design strategies in optimizing flow systems and enhancing performance [34, 41, 42]. Applying design automation to more complex process engineering systems, such as chemical reactors, remains a challenge due to the multidisciplinary nature of the field. A notable development in this area is the automated generation of flow reactors, introduced by Hou et al. [14, 43]. This approach employs a Python-based software tool that utilizes a library of pre-designed reactor modules, each corresponding to fundamental synthetic operations such as reactions, filtration, and separations. Users define their process requirements, and the tool automatically assembles an optimized reactor concept, streamlining the development process and reducing manual design efforts [14]. Another valuable approach in optimizing reactor design is the integration of machine learning and CFD to generate design variables for flow reactors [40]. In their study, one type of coiled reactor design is parametrized and evaluated using CFD simulations and multi fidelity bayesian optimization. Both studies highlight the effectiveness of computational methods in enhancing the reactor design process. However, both address individual stages of the design process rather

than coupling geometry generation, multiphysics evaluation, and optimization within a single integrated automation loop (see Table 2). Furthermore, the generation of reactor CAD models still requires substantial modeling expertise, which limits accessibility for chemists and chemical engineers. Applying design automation strategies to chemical reactors for decentralized systems also requires additional considerations, such as ensuring reactor safety under high-pressure conditions in addition to enhancing production rate. While design automation has been successfully implemented in various engineering fields, its application in energy systems remains largely unexplored. Moreover, integrating multiphysics simulations into reactor design automation introduces significant computational complexity, leading to prolonged simulation times and limiting practical feasibility. To address this challenge, we previously introduced a sequential parameter optimization workflow, incorporating finite element analysis (FEA) and CFD [44]. The tool presented in this work builds upon this workflow and extends it into an integrated design automation tool for methanol synthesis. The following section presents this methodology in detail.

3. Proposed design automation tool

This paper aims to develop a tool for the design and optimization of AM reactors based on a user-specified target methanol production rate, facilitating adaptation to various operational conditions, used catalyst type and renewable energy sources in decentralized systems with minimal human intervention. To achieve this, we have identified key requirements for an effective reactor design automation tool:

- **Mechanical strength:** Ensuring mechanical strength of the reactor under maximum operating pressures and temperatures.
- **Production rate optimization:** Reaching user-defined target methanol production rate by enabling precise control of residence time and temperature distribution based on reaction kinetics.
- **Design flexibility:** Developing a configurable tool that can adapt different reactor geometries to diverse operational conditions and varying renewable energy sources.
- **Computational efficiency:** Minimizing the time required for optimization calculations to streamline the design process and improving accessibility of advanced reactor development.

Given the complexity and variability inherent in methanol synthesis, and in alignment with the objectives of this study, we focus primarily on the commercialized CO_2 hydrogenation pathway, employing an industrial $Cu/ZnO/Al_2O_3$ (CZA) catalyst. Among the reactor concepts outlined in Section 2.1, the Lurgi reactor concept is selected as the reference design. This selection is motivated by its established industrial use and broad availability, which makes it particularly suitable for integration into KBE frameworks, thereby facilitating future design automation activities. To exploit the advantages of AM, including enhanced design flexibility and ease of prototyping, the Lurgi reactor concept is adapted and reformulated for compatibility with AM within the developed design automation tool (see Figure 2).

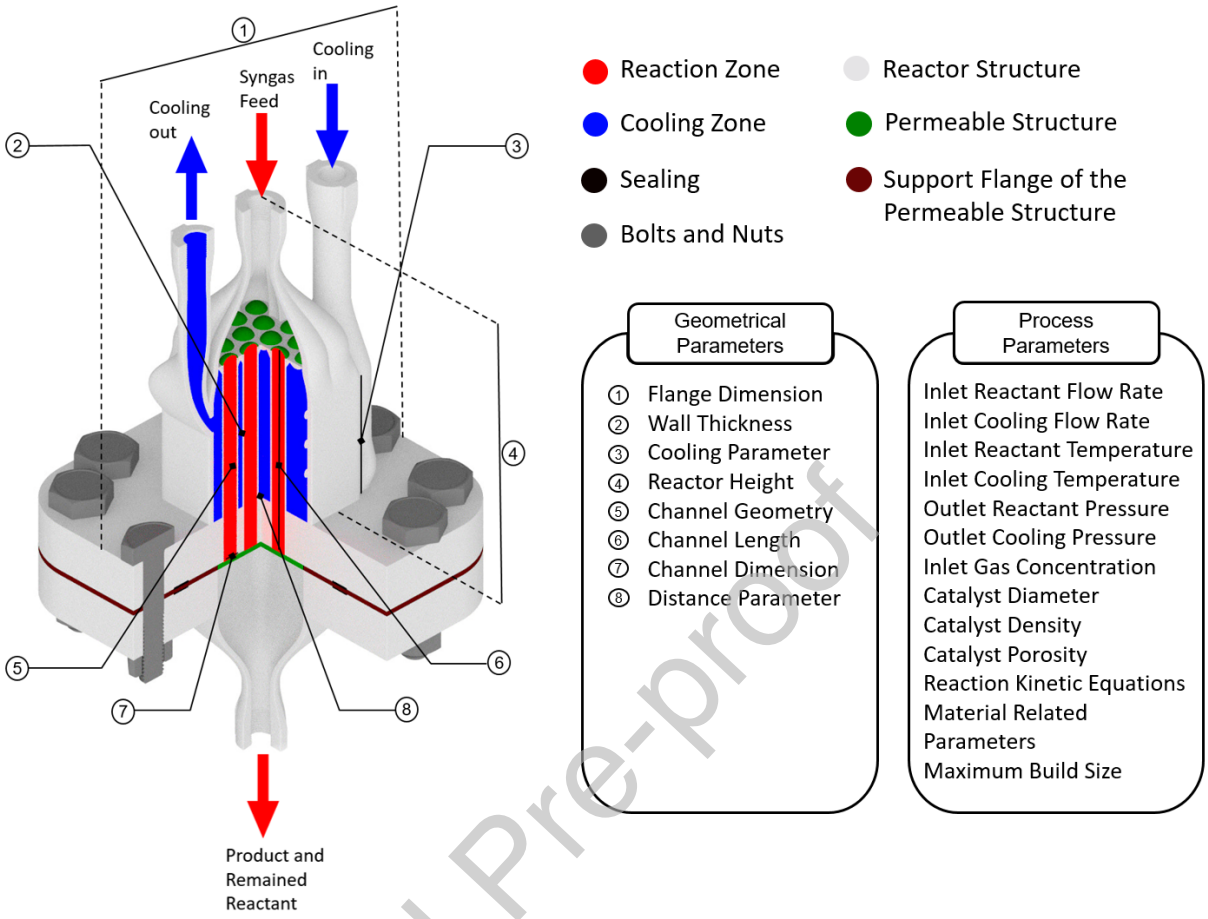

Figure 2: Schematic representation of the 3D-printed methanol synthesis reactor, illustrating key functional zones, structural components, and the associated geometrical and process parameters used in the design automation tool

The reactor is designed using algorithmic design techniques, based on a set of design elements defined in accordance with the DfAM principles outlined in Section 2.2. These elements are implemented in *Rhinoceros*® and enable the automated generation of varied reactor geometries. The data linkage between the design and simulation environments for the automated optimization activities is established through *Siemens HEEDS*, facilitating communication across different stages of the workflow. To address the complexity of multi-physics in reactor development for methanol synthesis in an automated manner, a sequential optimization methodology is implemented. The detailed implementation of this methodology is presented in our previous work [44]. To comprehensively represent the reactor behavior and guide the optimization process, an extensive set of geometrical and process parameters are defined (see Figure 2). These parameters reflect the key physical, thermal, and chemical characteristics of the system and form the foundation of the design space for subsequent optimization activities.

To develop a design automation tool that addresses all the requirements defined above, it is essential to thoroughly examine the methanol synthesis process and its associated parameters relevant to reactor design. A key consideration is the temperature dependent behavior of

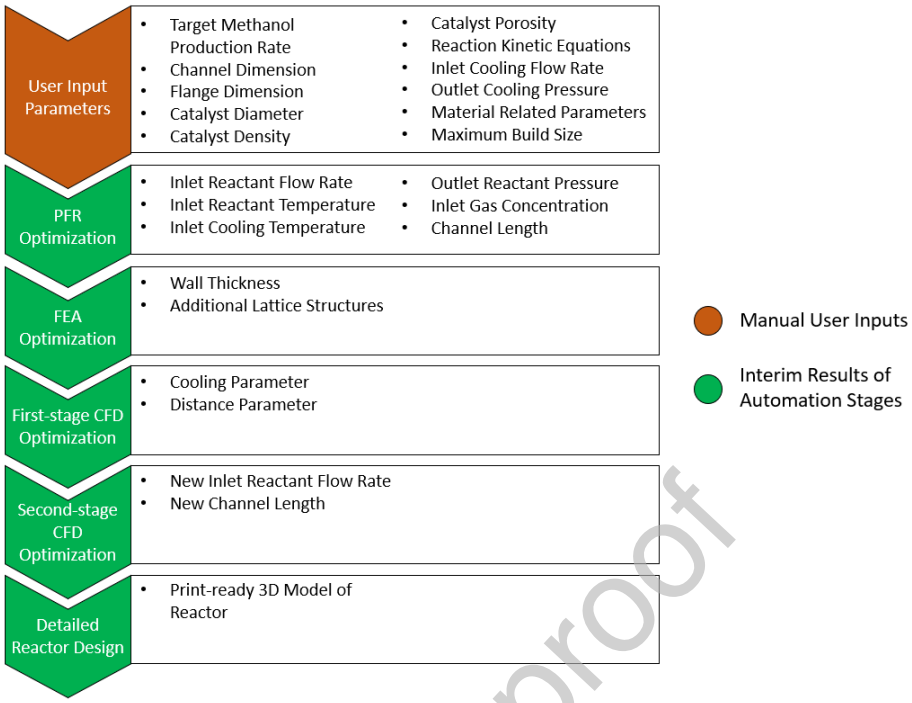

Figure 3: Workflow of the automated reactor design process in the proposed tool, illustrating the sequential optimization steps, from user input parameters through PFR, FEA, and CFD optimizations, to the generation of a print-ready 3D reactor model

the reaction system. At elevated temperatures, the RWGS reaction proceeds at a higher rate than CO_2 hydrogenation, whereas at lower temperatures, CO_2 hydrogenation becomes the dominant pathway, leading to increased methanol formation. However, lower temperatures may also impair catalyst activation, potentially limiting the overall methanol production rate [45, 46]. In addition to temperature effects, pressure plays a critical role in methanol synthesis. High operating pressures shift the chemical equilibrium toward methanol formation, thereby enhancing conversion. However, increased pressure also imposes greater mechanical loads on reactor components, necessitating careful consideration in the structural design to ensure operational safety [44]. These interdependent trade-offs between reaction kinetics, catalyst behavior, and mechanical constraints substantially increase the complexity of reactor development, underscoring the need for a multidisciplinary design and optimization approach.

Although the critical geometrical and process parameters are defined, as illustrated in Figure 2, certain inputs must be provided by the user due to limited information about the specific operational setup (see Figure 3). These inputs are not design variables. They represent the operational and hardware boundaries of the target facility and thereby define the design space within which the optimization is carried out. They include all catalyst-related properties, such as kinetic equations and physical characteristics, as well as material-dependent parameters like reactor and sealing materials. Additionally, operational setup factors, including the mass flow rate and medium of the cooling system and flange dimensions, require user input (see Figure 2). Furthermore, the build volume of the available AM machine

imposes limitations on reactor dimensions, directly impacting the feasibility of the proposed design.

Table 3: Objective, constraints, and optimization method of the four optimization stages, with design variables given in Figure 3

Stage	**Objective**	**Constraints**	**Optimization method**
PFR optimization	Minimize channel length at target production rate	Flow rate limit, CO formation limit	Bayesian optimization
FEA optimization	Minimize wall thickness	Stress $\leq f_d$, displacement ≤ 0.1 mm	Stepwise increase of wall thickness
CFD stage 1	Maximize methanol production rate	Geometric bounds	SHERPA algorithm
CFD stage 2	Achieve target methanol production rate	Convergence of production rate	Stepwise increase of inlet reactant flow rate and channel length

Building on these inputs, the tool comprises four sequential optimization stages and a final detailed design step. The PFR optimization first provides an initial dimensioning of the reactor channels and the reaction-side operating conditions. The reaction is modeled one-dimensionally along the channel axis using local reaction kinetics based on temperature, pressure, and molar flows (see supplementary information). These local conditions, however, are determined by the three-dimensional temperature and velocity fields within the reactor geometry. The PFR stage therefore assumes ideal cooling and defines the theoretical optimum. The FEA optimization then determines the required wall thickness. The geometry-dependent thermal behavior is then resolved in two CFD stages, which refine the cooling configuration and adapt the operating conditions to reach the target methanol production rate. Finally, the detailed design step generates the print-ready reactor model. The objective, constraints, and optimization method of each stage are summarized in Table 3, with the design variables given in Figure 3. The computational cost differs considerably between the stages: the PFR and FEA optimizations are computationally inexpensive, whereas the two CFD stages account for the majority of the total design time, since their cost depends on the number of channels and thus on the size of the generated mesh. The stages are described in detail in the following subsections.

3.1. Plug-Flow Reactor (PFR) Optimization

The design automation process begins with PFR calculations, which provide an initial dimensioning of the reactor channels under idealized conditions. These preliminary calculations serve to reduce computational cost by narrowing the design space and mitigating

uncertainties during the subsequent optimization cycle, thereby guiding the search toward a theoretical optimum. The following stages of the optimization workflow then refine this solution by adjusting key geometrical and process parameters. This approach aims to identify the optimal channel length and corresponding operating conditions for a given catalyst early in the development process. The methodology is based on established analytical models from the literature (see supplementary information).

Based on this foundation, the PFR optimization module processes user-defined inputs including the target methanol production rate, relevant reaction parameters and flange dimensions. The algorithm first estimates the maximum outer dimensions of the reactor and provides an initial prediction of the number of channels required. It then calculates the flow rate needed to meet the defined methanol production rate, assuming a fixed conversion target, and determines the channel length required to achieve this conversion using the specified reaction kinetics. As most kinetic models are based on the assumption of isothermal conditions without radial temperature gradients [16, 47, 48], the channel dimensions must be defined by the user to ensure the reactor geometry such as cylindrical channels or slit-like geometries remains consistent with these assumptions. In this stage, ideal cooling is assumed, meaning that the optimal reaction temperature is taken to be maintained throughout the catalytic bed, and both the reactor geometry and the reaction-side operating conditions are optimized under these idealized conditions. These results define the theoretical optimum that the subsequent CFD optimization stage, which incorporates a realistic cooling configuration and explicitly resolves heat transfer, aims to approach.

To enhance the optimization, a Bayesian algorithm, implemented using the *Skopt* library in *Python*, identifies the optimal combination of conversion, concentration, pressure, and temperature to reach target methanol production rate with minimal channel length in the catalytic bed. Minimizing the channel length enables a more compact reactor design, reduces the overall manufacturing costs associated with AM, and decreases the required catalyst volume. Bayesian optimization is selected because it is well suited to expensive black-box problems and identifies the optimum with comparatively few evaluations [49, 50]. To ensure process feasibility and safety, two constraints are integrated into the optimization: one limits the volumetric flow rate to remain within practical operational bounds, and the other restricts the CO formation to minimize undesirable side reactions. Due to the fast computation time enabled by analytical modeling, this stage allows for an efficient estimation of theoretical optima without the computational cost of multiphysics simulations. The algorithm is structured in a modular way, allowing users to easily substitute or update reaction kinetics based on different catalytic systems. The decision variable ranges, the objective formulation, and the number of evaluations are provided in the supplementary information. The full implementation is available in the GitHub repository [51]. At the conclusion of the PFR optimization module, a subset of the parameters are fixed for the following optimization modules, as illustrated in Figure 3.

3.2. FEA Optimization

Following the PFR optimization stage, a structural mechanics analysis is performed using *Abaqus* to optimize the reactor channel wall thickness. The objective is to minimize the wall thickness, thereby enhancing heat transfer within the reactor, while ensuring sufficient mechanical strength under the applied pressure loads. For the FEA, the optimum reaction

pressure obtained from the PFR optimization and the user-defined cooling-fluid pressure are used separately to calculate the corresponding test pressures according to DIN EN 13445-5, considering the selected reactor material and design temperature. The detailed pressure-load calculation is provided in the supplementary information. The optimization process is structured so that the algorithm initially assigns the minimum manufacturable wall thickness and progressively increases this value until the resulting stress remains within acceptable limits. To minimize computational costs, the simulation is carried out on a single representative channel, under the assumption that the pressure distribution from the reaction and cooling fluids is uniform across all channels (see Figure 4). An automated mesh generation process is implemented in *Abaqus* via a macro script. Mesh sensitivity is evaluated by progressively coarsening the tetrahedral mesh while monitoring the resulting stress, and the coarsest mesh for which the stress shows no relevant change is selected, thus achieving a balance between computational efficiency and accuracy.

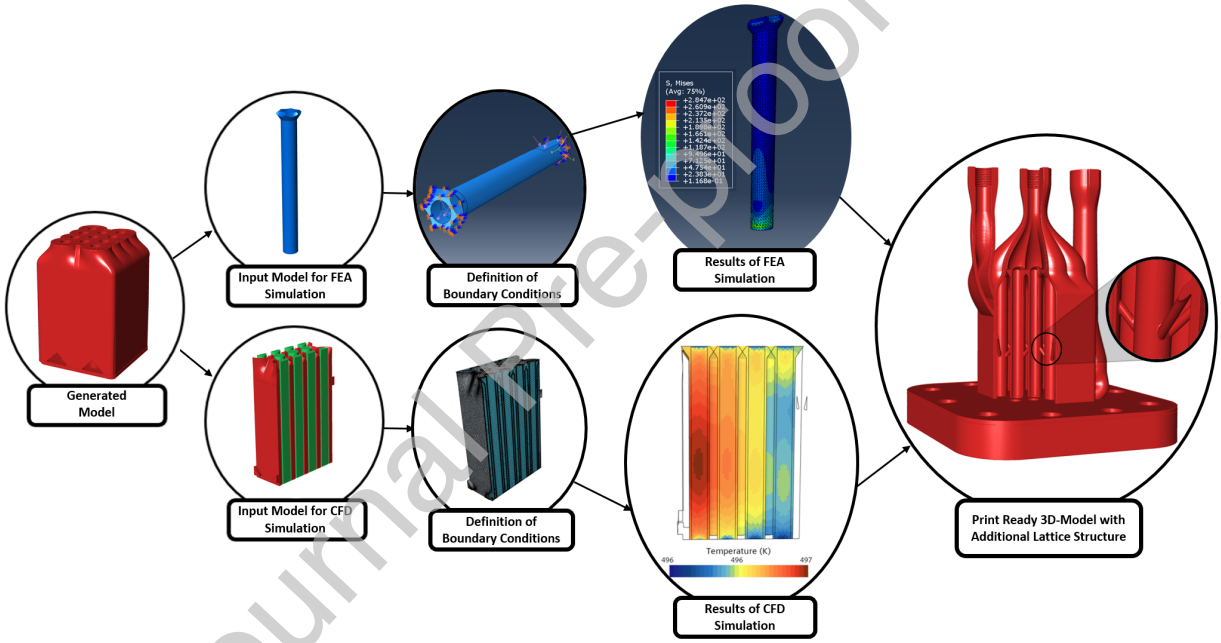

Figure 4: Illustration of a single CFD or FEA simulation workflow and the generation of a print-ready 3D-Model with additional lattice structure (adapted from [44])

A linear static structural simulation is conducted to analyze the mechanical behavior of the reactor channel under operating conditions. The interfaces between the reactor channel and its main body are defined as fixed supports. Additionally, internal and external pressures, representing reaction and cooling fluid pressures, respectively are incrementally applied as mechanical loads in multiple analysis steps to accurately simulate the operational scenarios. Stainless steel 316L is chosen as the simulation material, as its use is predefined within the scope of this study.

$$f_d = \max\left[\frac{R_{p1.0/T}}{1.5};\ \min\left(\frac{R_{p1.0/T}}{1.2};\ \frac{R_{m/T}}{3}\right)\right] \tag{4}$$

The maximum acceptable stress level (f_d) is defined based on the use of stainless steel

316L as the reactor material, in accordance with the DIN EN 13445-3 standard. According to this norm, f_d is determined using the proof strength at 1.0% plastic strain at the operating temperature ($R_{p1.0/T}$) and the ultimate tensile strength at the operating temperature ($R_{m/T}$). In the FEA model, the representative reactor channel is mechanically constrained at its connection points to the surrounding reactor body. One side of the model is fixed, while the opposite side is constrained using a symmetry boundary condition. This represents the support that the channel receives from the surrounding reactor structure and prevents unrealistic free movement of the model. The reaction-side and cooling-side pressures are applied as individual pressure-load cases to the corresponding channel surfaces, and the wall thickness is evaluated based on the resulting stresses. Additionally, structural displacement is evaluated during the FEA optimization. If displacement exceeds 0.1 mm, the algorithm automatically incorporates additional lattice structures into the reactor body to enhance stiffness (see Figure 4). The displacement threshold of 0.1 mm is introduced as a conservative stiffness-related functional limit, since excessive displacement in thin-walled, elongated parts indicates insufficient structural stiffness and can lead to increased mechanical stresses that cannot be efficiently reduced only by increasing the wall thickness [52]. This approach enables determination of the maximum permissible unsupported channel length based on mechanical stresses. In subsequent stages of the automation tool, this information guides the placement of lattice reinforcements when the channel length exceeds the allowable limit. Once the minimum acceptable wall thickness is determined, the FEA optimization module concludes, and the tool proceeds to the CFD optimization stage.

3.3. CFD Optimization

In contrast to the PFR optimization, this stage incorporates the effects of heat transfer and flow behavior, along with reaction kinetics, to evaluate the reactor's performance under more realistic conditions. The CFD simulations are employed to assess different design variants and identify the optimal set of geometrical parameters that most closely achieve the theoretical optimum previously defined in the PFR stage. To generate reliable initial designs for the CFD simulations, an automated meshing process is implemented in *STARCCM+*, utilizing polyhedral meshes with prism layers at the boundaries to capture near-wall effects and thermal gradients accurately. To further reduce computational cost, symmetry in the reactor geometry is exploited, allowing for simulation of only a representative section of the domain (see Figure 4). The base size is progressively increased while monitoring the methanol production rate, and the coarsest mesh for which the production rate shows no relevant change is selected and applied unchanged in the automated workflow. Since the absolute cell count follows from the size of the generated geometry, the mesh is defined by the base size and the prism layer settings rather than by a fixed cell count.

In the CFD model setup, the reactor body is assigned the material properties of stainless steel 316L, while the cooling fluid is defined using the thermophysical properties of *Thermal HL60* provided by *Julabo*. The catalytic bed is modeled as a porous medium, and the chemical reaction is implemented using a user-defined kinetic expression within the Eddy Break-Up framework. Detailed surface reaction kinetics are not resolved, since methanol synthesis under the considered operating conditions is equilibrium-limited and the model targets the conversion field rather than surface coverages. A global kinetic description is therefore sufficient and consistent with established reactor-scale CFD studies of methanol

synthesis [8, 45], while considerably reducing computational demand. To represent the thermal behavior of the system accurately, Segregated Energy Models are used to define the energy balance in both the reactor body and the catalytic bed. Segregated solvers compute momentum, energy, and continuity equations sequentially, offering greater numerical stability and reduced computational cost compared to fully coupled models in cases where compressibility effects are negligible [53]. In particular, an additional segregated energy model is applied to the porous media to more accurately capture heat transfer within the catalyst region. The simulation accounts for conduction through the reactor body and catalyst, as well as convective heat transfer between the cooling fluid and reactor body, and between the reaction fluid, reactor body, and catalyst.

Due to the varying behavior of classical convergence criteria in response to different input parameters within an automated simulation setup, a customized stopping criterion is defined. This criterion ensures that the simulation terminates when the methanol production rate shows no significant change over time. As shown in Equation 5, the convergence check is based on the absolute change in methanol production rate over the last 20 iterations, denoted by δ and is compared against a threshold defined as a fraction (κ) of the target methanol production rate ($\dot{V}_{\mathrm{MeOH,target}}$).

$$\delta < \frac{\dot{V}_{\mathrm{MeOH,target}}}{\kappa} \quad \text{where} \quad \kappa = 10000 \tag{5}$$

The value of $\kappa = 10000$ is selected because the resulting tolerance, approximately 10^{-5} in the present simulation setup, corresponds to a very small change in methanol production rate and is therefore expected to have a negligible practical effect on the reactor performance. In addition, evaluating the change in production rate over the last 20 iterations ensures that the criterion is based on a stable trend. A smaller κ value allows the simulation to terminate earlier, potentially at the cost of accuracy, while a larger κ increases accuracy but also extends the required computational time. The value of κ can be tuned according to the specific requirements of the optimization problem, enabling a flexible trade-off between computational efficiency and solution precision. If the stopping criterion is not satisfied, the simulation continues until it reaches a maximum of 3000 iterations and then it stops. Further details regarding the CFD model are provided in the supplementary information.

In the first stage of the CFD optimization, two design parameters, cooling parameter and distance parameter, are optimized using *SHERPA* (Simultaneous Hybrid Exploration that is Robust, Progressive and Adaptive) optimization algorithm provided by *Siemens HEEDS* (see Figure 3). The cooling parameter defines the flow configuration within the reactor(see Figure 2). Depending on its assigned value (0.0, 0.5, or 1.0), the flow pattern is configured as counter-current (0.0), cross-flow (0.5), or co-current (1.0). The distance parameter controls the spacing between adjacent channels, thereby influencing the number of channels (N) and the length of individual channels indirectly, while keeping the total catalyst volume constant. As illustrated in Figure 5, varying the distance parameter enables indirect control over these geometrical characteristics. To illustrate this, the lab-scale reactor is considered as an example, with an outer dimension of 22 mm, a channel radius (r) of 3 mm and a wall thickness (s) of 1.2 mm obtained from the FEA optimization. For a distance parameter (DP) of 0.5 mm, the channel pitch (DP + s + r) amounts to 4.7 mm, and Equations 7 and 8 yield 4 and 5 for the horizontal and vertical directions, respectively. The channels in adjacent

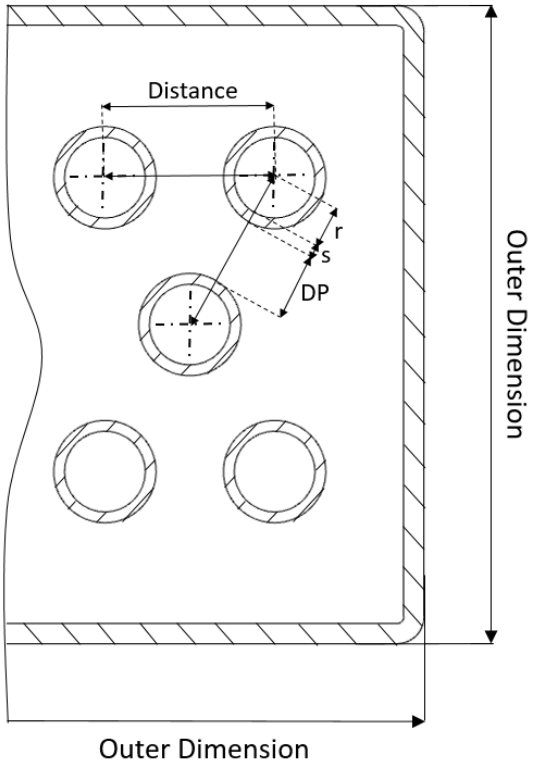

$$\text{Distance} = 2 \cdot (s + r) + \text{DP} \tag{6}$$

$$N_{\text{horizontal,1}} = \left\lfloor \frac{\text{Outer Dimension}}{\text{DP} + s + r} \right\rfloor \tag{7}$$

$$N_{\text{vertical,1}} = \left\lfloor \frac{\text{Outer Dimension}}{(\text{DP} + s + r) \cdot \cos(30°)} \right\rfloor \tag{8}$$

$$N = N_{\text{vertical}} \cdot N_{\text{horizontal}} - \left\lfloor \frac{N_{\text{vertical}}}{2} \right\rfloor \tag{9}$$

Figure 5: Geometrical definition of the channel arrangement within the reactor cross-section, relating the distance parameter (DP), wall thickness (s), and channel radius (r) to the resulting number of channels (N) at constant catalyst volume

rows are offset by half of the horizontal spacing, so that the vertical distance between the rows is reduced by the factor cos(30°) used in Equation 8. Because of this offset, every second row accommodates one channel less within the same outer dimension. Applying this arrangement to the represented cross-section results in a total of 18 channels. Increasing the DP to 2.5 mm reduces the total number of channels to 8, and since the total catalyst volume is kept constant, this reduction is compensated by a corresponding increase in the length of the individual channels. This provides a basis for further refinement of the reactor's channel layout, building on the fixed parameters determined in the PFR optimization stage. Following the first stage of the CFD optimization, the optimal configurations for the cooling and distance parameters are identified.

In methanol synthesis, the influence of the RWGS reaction causes a discrepancy between the formation rates of water and methanol, making it difficult to directly achieve the target methanol production rate (see Equations 2 and 3). To address this, a second stage of CFD optimization is incorporated into the design automation tool. This stage iteratively adjusts the inlet reactant flow rate and the channel length to converge toward the user-defined methanol production rate. The second stage terminates automatically once the specified production rate is achieved. If the target production rate remains unmet despite reaching the upper limits of flow rate and reactor size, imposed by operational and hardware constraints, the tool returns an error message indicating that the target production rate is infeasible

under the given conditions.

Only after the methanol production rate has been successfully achieved, all geometrical and process parameters defined in Figure 2 are fixed, and the detailed reactor design phase is initiated, culminating in the generation of a print-ready 3D model for reactor fabrication. In contrast to the simplified input models used during numerical simulations, the final reactor design is based on the fixed geometrical parameters and developed in full detail, including the design of appropriate connections to the piping system of the operational plant. At the moment, only G1/8" connections have been implemented, as they have been sufficient for this application. However, the developed design automation tool is structured to be extendable and can be adapted to incorporate other connection types as needed.

4. Experimental Results

To demonstrate the effectiveness of the proposed design automation tool, it is essential to validate the simulations on which it relies. These simulations provide efficiency estimates that serve as the basis for decision-making within the tool. Validating the models and ensuring accurate selection of reactor geometries are therefore critical to confirming the tool's reliability. To minimize cost and leverage the rapid prototyping benefits of AM reactors, both FEA and CFD simulations are validated using lab-scale prototypes manufactured via the PBF-LB/M process on a *DMG MORI Realizer SLM125* machine, using the qualified standard parameter set for stainless steel 316L. The design rules summarized in Table 1 correspond to this parameter set. The prototypes are intentionally kept below the volume threshold requiring formal certification by a notified body under the Pressure Equipment Directive (PED). According to PED 2014/68/EU, pressure equipment classified under fluid group 1, such as methanol synthesis reactors, with an internal volume below 1 liter are exempt from intensive certification procedures and can be operated in accordance with established engineering practice [54]. Accordingly, the FEA-optimized prototype is subjected to pressure testing for structural validation. Additionally, methanol synthesis experiments are conducted to validate the CFD model under relevant operating conditions.

4.1. Manufacturing and Leak/Pressure Tests

In the reactor design, process integration is defined as a primary objective and is largely implemented to minimize the number of sealing interfaces. The use of fewer components reduces potential leakage points, especially in high pressure systems and enhances operational safety. However, despite the advantages of process intensification enabled by AM, direct access to the catalyst zone remains essential. Due to challenges in achieving uniform filling of microchannels with catalyst, a practical solution is required. Therefore, a flange connection is incorporated into the reactor design to allow direct access for catalyst loading (see Figure 6). This connection also enables the catalyst to be replaced or refilled without modifying the reactor body.

After manufacturing, the reactor connections are post-processed to accommodate standard metallic fittings and sealing gaskets from *Swagelok*, ensuring a leak-tight connection to the test rig. Hybrid manufacturing greatly reduces post-processing effort by eliminating the need for support structures through direct additive fabrication on a conventionally

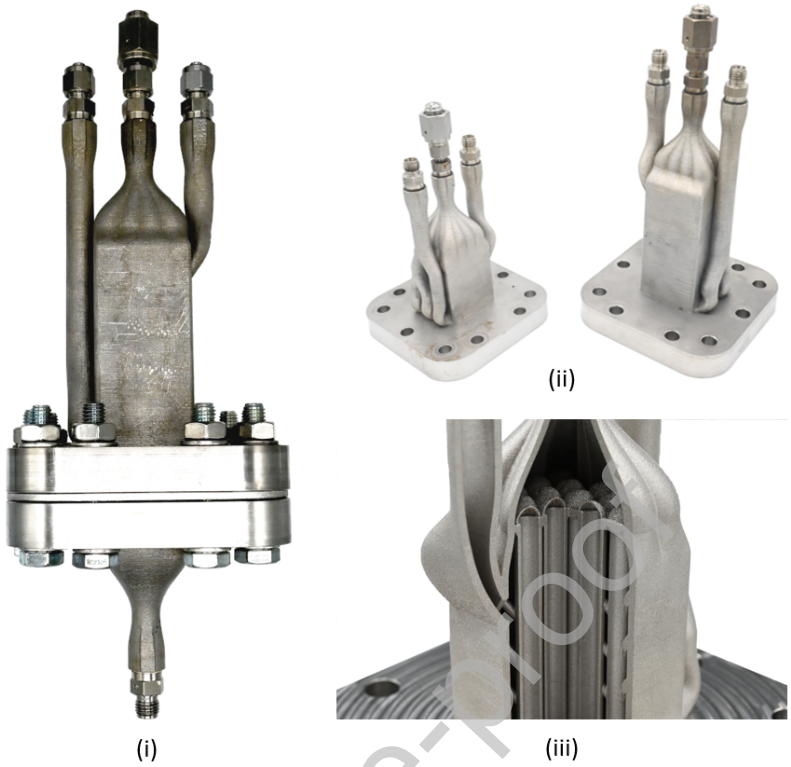

Figure 6: Additive manufactured reactor components for experimental tests: (i) Assembled configuration, (ii) manufactured reactor prototypes, and (iii) internal design of the reactor with permeable catalyst holder

produced flange. To validate the proposed design automation tool without introducing additional complexity into the system, a multitubular channel design is used. Different reactor configurations containing the same amount of catalyst are tested to ensure that the effects of geometrical parameters are accurately captured by the simulations integrated within the design automation tool (see Figure 6). To generate these configurations, the cooling and distance parameters described in Section 3 are systematically varied. Two reactor prototypes are manufactured, each with a different distance parameter set to 0.5 mm and 1.0 mm, respectively. For each prototype, the cooling parameter is varied by modifying the flow arrangement of the cooling fluid between co-current and counter-current operation, resulting in the four reactor configurations used for the validation.

The manufactured prototypes are first tested for leak-tightness following the post-processing of the reactor connections. Leakage tests are conducted using a *PhoeniXL* detector provided by *Leybold*. The prototypes are connected to the leak detector and examined using helium as the test medium. Gas-tightness is confirmed by verifying that leakage rates remain below $1 \times 10^{-8}\,\mathrm{mbar\,L\,s^{-1}}$, a threshold accepted for gas-tightness [55, 56].

The test pressure for the pressure tests is calculated according to the same pressure-test procedure used for defining the FEA pressure loads, as described in the supplementary information. The maximum possible operating pressure is set to 50 bar and the maximum temperature to 300°C. Based on these conditions, the calculated test pressure is rounded upward to 105 bar. Accordingly, the prototypes are subjected to pressure testing at 105 bar

using water as the test medium, with test equipment provided by *Sitec*. All tested prototypes successfully withstand the applied pressure, confirming their suitability for operation under the defined conditions.

4.2. Reaction Experiments and CFD Validation

To ensure the reliability of the CFD simulations integrated into the proposed design automation tool, methanol synthesis experiments are conducted for validation. This step is essential for verifying the accuracy of the optimization workflow in achieving the target methanol production rate.

The prototypes are loaded with an industrial CZA catalyst following the approach demonstrated by Metzger et al. [25]. In this method, the catalyst is filled into the channels by inverting the reactor. In this position, the catalyst is loaded into each channel, where it is temporarily held in place by an integrated additively manufactured frit. After the channels are filled, a conventionally manufactured frit is assembled onto the reactor together with a graphite-based sealing element to secure the catalyst. The remaining flange is attached to complete the assembly (see Figure 6). Once sealed, the reactor is subsequently returned to its upright position. This method ensures uniform catalyst distribution while allowing access for maintenance or refilling.

Each prototype is charged with 21.5 g of catalyst and 9 g of silicon carbide (SiC). The catalyst and the SiC are weighed individually for every channel and filled in equal amounts, so that all channels of a prototype contain the same catalyst mass and bed structure. The SiC is split evenly to fill the upper and lower channel sections, while the central portion contains only catalyst, ensuring undiluted contact with the reactant flow. The reaction is modeled using the kinetic expressions provided by Lacerda de Oliveira Campos et al. [16], which serve as the basis for experimental validation of the CFD simulations. The kinetic model is selected because the same industrial catalyst is used in the experiments, minimizing potential inconsistencies between the simulated reaction behavior and the experimental performance. It should be noted that the employed kinetic model neglects the CO hydrogenation pathway (Equation 1), focusing solely on CO_2 hydrogenation and the RWGS reaction. This is appropriate for the CO_2 rich feed used in the experimental campaign, where CO is formed only in situ via RWGS (Equation 3) and remains at low concentration. The model is therefore not suitable for CO-rich feeds or for catalysts developed for such feeds without revalidation of the kinetics for the respective system. Since the tool allows the kinetics to be substituted, this limitation concerns the kinetic model rather than the workflow itself. For consistency, the catalyst reduction procedure described by Lacerda de Oliveira Campos et al. [16] is followed. The complete reduction process takes approximately 11 hours for each prototype.

Model validation is performed by comparing the outlet volume flows of CO_2, CO, and H_2 between simulations and experimental results. This approach follows established validation practices in the field, where outlet species compositions are commonly used to assess the agreement between model predictions and experimental observations [16, 47, 48]. The comparison is carried out on a volumetric flow basis, as the flows combine the measured composition with the measured total outlet flow and therefore reflect the quantity that determines the methanol production rate targeted by the design automation tool. Since the stoichiometric matrix of the main reactions in methanol synthesis has a rank of two, only

two component balances are theoretically required to define the system [48]. Among these, CO_2 and H_2 are the most critical reactants in methanol synthesis via CO_2 hydrogenation and thus serve as the primary basis for model evaluation. CO is also included in the validation to complement the comparison, but the accurate representation of CO_2 and H_2 is of particular importance for assessing the fidelity of the CFD model.

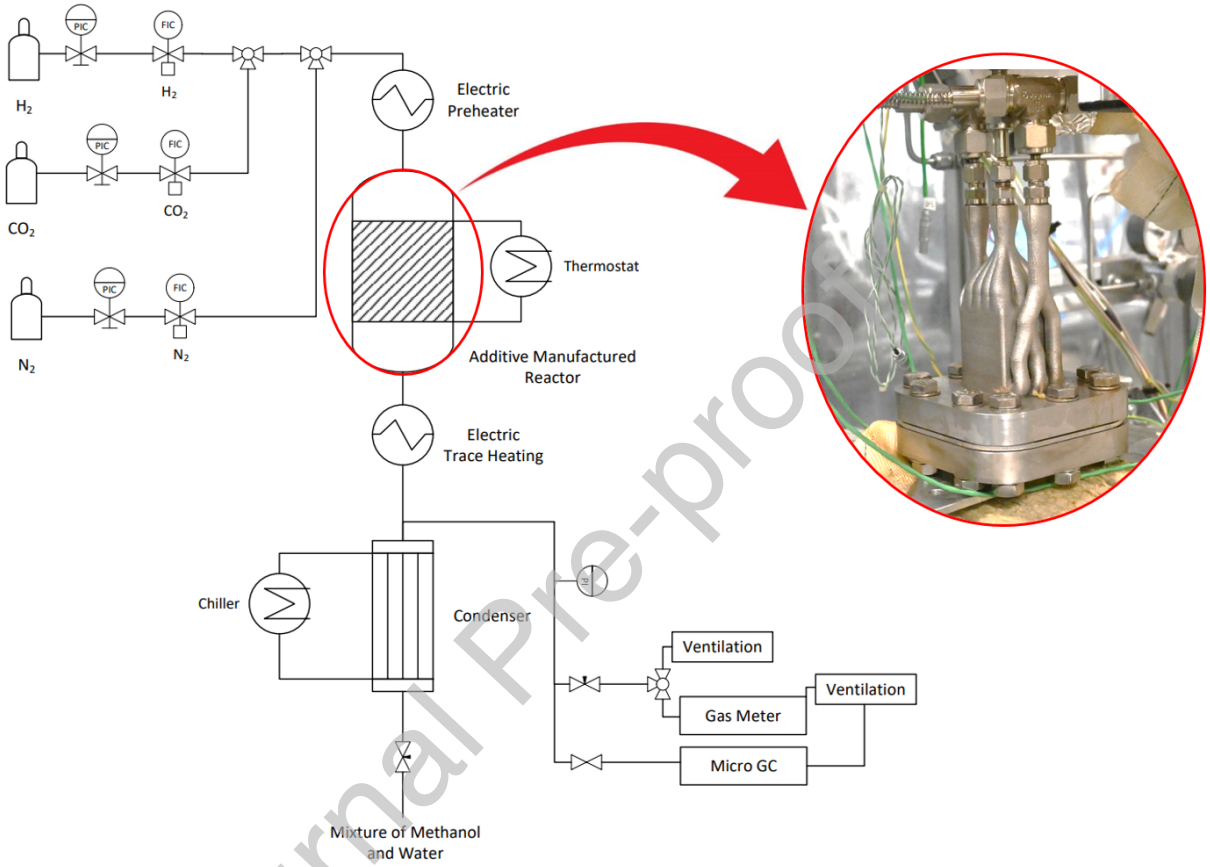

Figure 7: Schematic of the experimental setup for methanol synthesis, highlighting the integration of the additively manufactured reactor. The detailed view shows the assembled reactor installed within the test bench

The lab-scale test rig used for the reaction experiments is connected to gas supplies of CO_2, H_2 and N_2. CO_2 and H_2 serve as reactants for methanol synthesis, while N_2 is used to pressurize the system (see Figure 7). During operation, the process conditions of the reactants are controlled using pressure regulators from *Swagelok* and mass flow controllers (MFC) supplied by *Brooks*. The reactants are mixed within the piping system and preheated to the desired reaction temperature using electrical heaters provided by *Horst* and *Ihne & Tesch GmbH*. Temperature monitoring is performed at several locations throughout the test rig, particularly upstream of the reactor, using thermocouples from *Conatex*. Once preheated, the gas mixture enters the reactor where the methanol synthesis reaction occurs. Upon exiting the reactor, the product stream is passed through a heat exchanger to condense and separate liquid products, such as water and methanol, from the remaining unreacted gases. The composition of the remaining gas mixture is then analyzed using an *Agilent*

490 Micro Gas Chromatograph, and its flow rate is measured using a gas meter provided by *Intergaz*. During the testing process, the MFCs are calibrated once prior to the first reaction test, while the Micro Gas Chromatograph is calibrated before each experiment for the individual prototype. Further details regarding the kinetic model, the calibration procedures and the overall testing process are provided in the supplementary information.

The prototypes are operated at 41 bar and 220°C with an initial feed composition of H_2 and CO_2 at a 3:1 volume ratio. For each of the four reactor configurations discussed in Section 4.1, the total inlet flow rate of the reactants is varied at 450, 600, 900, 1200, and 1500 mL_s/min. Since the underlying reaction kinetics are adopted from an independently validated model calibrated over a wide range of operating conditions, including varying pressures, temperatures, and feed compositions [16], the present experimental campaign focuses primarily on the effects of flow rate and geometry. As direct determination of the cooling fluid mass flow rate and the catalyst wall heat transfer coefficient is not possible, these parameters are estimated by iteratively adjusting their values until the simulated outlet volume flows agree with the measurement for selected experimental operating conditions. Based on this calibration, the wall heat transfer coefficient of the catalyst channel is set to 5 $W/m^2 \cdot K$, and the mass flow rate of the cooling fluid is defined as 0.0574 g/s to achieve consistency with the measured outlet volume flows. Both values are subsequently kept fixed and applied unchanged across all reactor configurations and inlet flow rates, comprising 19 averaged data points in total (see supplementary information). Although this approach avoids configuration-specific refitting, the calibrated values may partly compensate for inaccuracies in other model components and should therefore be regarded as effective calibration parameters.

The comparison demonstrates good overall agreement between experimental and simulated data (see Figure 8). For CO_2 and H_2, all data points lie within the 20% deviation band across the full range of tested flow rates, with the root mean square error (RMSE) values of 3.67 and 34.15 mL_s/min and mean absolute error (MAE) values of 3.01 and 30.80 mL_s/min, respectively. Since the outlet flows of these species span 81 to 313 mL_s/min for CO_2 and 243 to 1087 mL_s/min for H_2, these deviations are small in relative terms. For CO_2, the deviations scatter in both directions without a systematic trend, so the simulated CO_2 conversion agrees closely with the experiment over the entire flow range. The H_2 outlet flow, in contrast, is slightly overpredicted in all tested cases, indicating that the simulation marginally underestimates the H_2 consumption. The offset remains well within the 20% deviation band and does not affect the ranking of the tested reactor configurations. For CO, the simulation slightly overpredicts the outlet flow, suggesting a marginal overestimation of the RWGS reaction extent in the model. However, the effect of this CO prediction difference is very limited due to the low amount of CO in the system. Alternatively, the discrepancy may also stem from uncertainties in the experimental measurement, which are more pronounced at such low concentration levels.

5. Discussion

5.1. Effect of Geometrical Parameters and Up-scaling Scenarios

While reactor efficiency is influenced by process parameters, geometrical optimization also plays a critical role, particularly in determining the effectiveness of heat and mass transfer

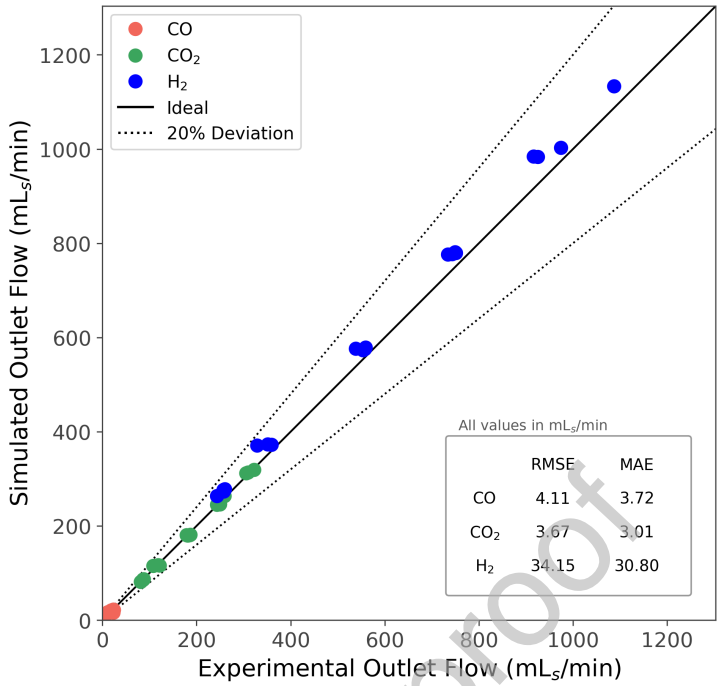

Figure 8: Parity plot of simulated and experimental outlet volume flows of CO, CO_2, and H_2 for all tested reactor configurations and inlet flow rates; full test data are available in the supplementary information

within the reactor. Therefore, achieving a target methanol production rate requires the joint optimization of both process and geometrical variables. The proposed design automation tool addresses this need by integrating geometry-based optimization into the overall reactor development workflow. In small, lab-scale reactors, heat transfer is typically near ideal due to favorable surface-to-volume ratios. However, as reactor size increases, thermal management becomes significantly more complex. This challenge is closely tied to the scale-up problem: when the required heat removal rate is expressed in absolute terms, it increases substantially from lab to commercial scale, a relationship characterized by the scale-up ratio [57]. As this ratio grows, ensuring efficient heat and mass transfer becomes increasingly difficult, underscoring the importance of geometry-aware design at industrial scales.

To illustrate the role of geometrical parameters and demonstrate the applicability of the proposed tool in up-scaling scenarios, this study presents two reactor development studies carried out with the design automation tool: One for a lab-scale reactor targeting a methanol production rate of 0.125 L/day, and another for a container-scale reactor designed to produce 50 L/day. To ensure realistic and scalable results at the container scale, several key parameters are adjusted prior to initiating the automation process. The inlet cooling flow rate is increased from 0.0574 g/s to 0.574 g/s, assuming that a correspondingly larger cooling system is available at this scale. Additionally, the maximum allowable inlet reactant flow rate is raised from 1 L/min to 450 L/min to reflect practical operating conditions at this scale. The manufacturing size constraint is also expanded from 120 × 120 × 200 mm^3 to 350 × 350 × 500 mm^3, corresponding to the build volumes of widely available PBF-LB/M systems. These parameters represent the operational and hardware boundaries of the target facility rather

than design variables, and are therefore specified as user inputs, as defined in Section 3. Since these inputs define the operational and hardware boundaries of the target facility, the reliability of the generated design depends directly on their accuracy, and unrealistic inputs will accordingly lead to unrealistic designs. Apart from the target methanol production rate and the three parameters listed above, all remaining parameters are kept identical in both studies. The channel diameter is fixed at 6 mm in both reactor development studies, since the employed kinetic model assumes the absence of hot spots within the channel, and this condition is experimentally confirmed for this diameter at lab scale. Retaining small channel diameters at container scale remains realistic, as structured reactors with intensified channels are the main application domain for AM at this scale. The adaptation to the container scale requires no manual design activity, as the geometry generation, the structural verification and the optimization of the geometrical and process parameters are carried out by the tool without further intervention.

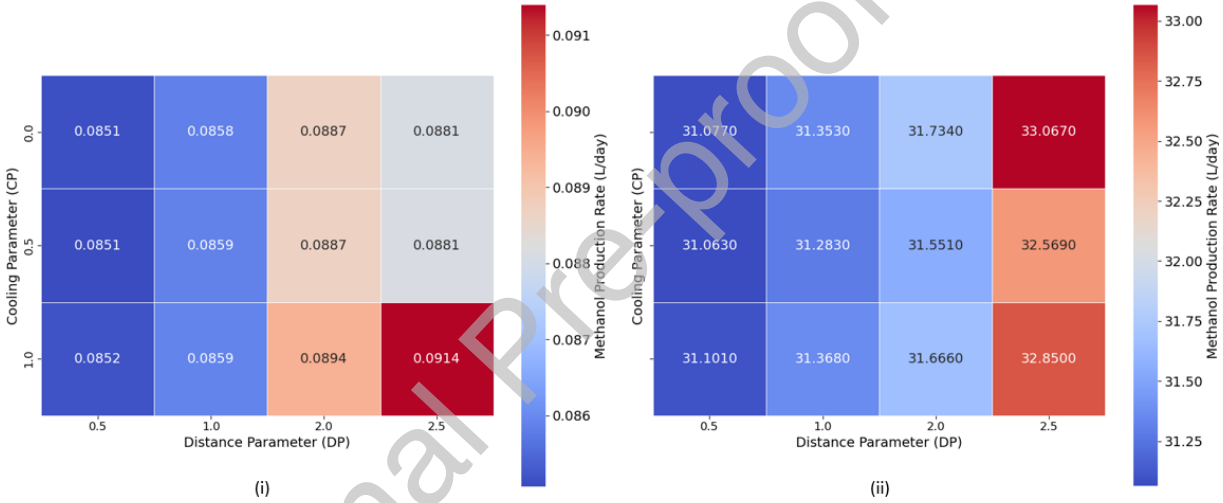

Figure 9: Effect of cooling and distance parameters on methanol production rate at (i) lab and (ii) container scale, showing how the influence of both parameters changes with reactor scale

In the design study of the lab-scale reactor, the proposed design automation tool successfully generates a print-ready, optimized reactor model within approximately 105 minutes. By the third iteration of the second stage of CFD optimization, the reactor achieves the target methanol production rate. Results from the first stage of CFD optimization (see Figure 9), which focuses on refining two critical geometrical parameters, namely the cooling and distance parameters, indicate that the distance parameter has a considerable influence on methanol production rate. Since the total catalyst volume and the inlet reactant flow rate are kept constant when the distance parameter is varied, the residence time in the catalytic bed remains unchanged, and the observed differences in production rate cannot be attributed to increased contact time. Instead, a higher value redistributes the same catalyst volume into fewer and longer channels, so that both the heat-transfer area and the heat released per channel increase. The resulting change in the balance between heat release and heat removal alters the axial and radial temperature gradients within the catalytic bed. The CFD results indicate that these gradients become more favourable at larger distance parameter values,

which is reflected in the higher methanol production rate. In contrast, the cooling parameter has a comparatively minor effect, particularly in designs with small distance parameter values. This limited effect is probably due to small values of the distance parameter, which leads to reduced channel heights. Under these conditions, the effect of flow direction on heat transfer becomes negligible in small-scale reactors.

As shown in Figure 9, the influence of geometrical parameters becomes significantly more pronounced at larger scales. At the container scale, variations in methanol production rate occur at the liter-per-day level, which is critical for overall reactor performance. Here the greater absolute heat release and the longer channels increase the axial temperature change of the cooling fluid, so that the flow arrangement establishes distinct axial temperature profiles in the bed and the cooling parameter becomes relevant. Consequently, optimizing geometrical parameters becomes essential in the design of pilot- and commercial-scale reactors. The proposed design automation tool facilitates the automated optimization of both geometrical and process variables, addressing scale-up challenges while significantly reducing development time. In the container-scale design study, the tool generates an optimized reactor design within approximately 27 hours, during which it runs automatically and requires no user interaction. This remains practical compared to conventional development cycles, where the repeated CAD generation, simulation setup, and design iterations occupy engineering time. The computational effort is nevertheless considerable and increases with the reactor size, so that it would become a limiting factor for substantially larger reactors or for the evaluation of several channel concepts. The target methanol production rate is reached in the fourth iteration of the second stage of CFD optimization, compared to the third iteration at lab scale. The considerably longer design time is therefore not caused by a higher number of optimization iterations, but by the cost of the individual design evaluations. The larger build volume permits a higher number of channels, which increases the complexity of the generated geometry and the size of the resulting mesh, so that both the geometry generation and the CFD evaluation become more expensive per iteration.

From these two design studies, some general design guidelines can be derived for this reactor concept. Larger distance parameters give higher methanol production at both scales, with the best result at the upper bound of the investigated range of 0.5 to 2.5 mm. The effect matters most at larger scales, where this variation corresponds to a gain of about 2 L/day. For this reactor concept and the given operating conditions, the cooling parameter is a secondary design variable, since it only becomes relevant once the channels are long enough for the coolant temperature to change noticeably along the flow path.

5.2. Further improvements

The proposed design automation tool provides substantial support to chemical engineers in defining reactor geometry and sizing for decentralized methanol production. The challenge of up-scaling can be mitigated through the increasing adoption of automated design systems that optimize both reactor geometry and process parameters within a digital environment. From an energy efficiency perspective, our findings show that tailoring geometrical parameters to application-specific requirements can significantly reduce reliance on external high-power cooling or heating systems, thereby enhancing overall system efficiency. As part of future work, the optimized reactors may be operated using more cost-effective cooling solutions, such as water vapor systems commonly employed in industrial settings, without

compromising methanol production levels. Beyond reactor design optimization, the proposed design automation tool can serve as a foundational step for the systematic generation of training data for future data-driven applications. Each optimization run records the geometrical parameters, the operating conditions, and the resulting performance indicators such as methanol production rate, pressure drop across the channel, and axial and radial temperature differences within the channels, together with the underlying CFD and FEA results. Since every run follows the same workflow, these records are consistent and can be collected over time. Once enough data has been gathered for a given catalyst and reactor concept, it could be used to train surrogate models, for example random forests or Gaussian process regression. Such models could then replace part of the simulation effort in later design studies for the same reactor concept, further shortening the development time. However, the reliability and performance of the proposed tool strongly depend on the underlying reaction kinetics. The evaluation carried out in this work indicates that the kinetic model presented in [16] offers higher fidelity for the used industrial catalyst than the widely used model in [58]. Nevertheless, during model selection, faster numerical convergence is observed with the kinetic model from [58], which may accelerate the automation process. As this model is not validated for the employed catalyst within this work, the observation is qualitative and a quantified comparison would require both models to be validated and evaluated under identical conditions. Furthermore, the approval of commercial reactors for industrial application by notified bodies may require additional structural testing. While the lab-scale prototypes used in this work remain below the volume threshold for formal certification under PED 2014/68/EU, larger reactors such as the container-scale design exceed this limit and are subject to stricter requirements. Therefore, the design automation tool must be adapted to incorporate the specific testing protocols mandated by these regulatory authorities. The container-scale reactor is moreover investigated as a design study only, without manufacturing or experimental testing. The transferability of the validated simulation models to this scale therefore remains to be confirmed. Similarly, fouling and the evolution of pressure drop over long-term operation are not investigated in this work and remain outside its scope. The same applies to the flow distribution between the channels, which is assumed to be equal at container scale.

For specific operational requirements, the optimum reactor geometry can vary significantly. The proposed design automation tool is capable of handling different channel concepts without the need to manually build new CAD models from the beginning, by reusing modular design elements as described in [44]. As illustrated in Figure 10, the tool accommodates various channel configurations. However, each geometry must still be individually optimized by following the workflow presented in Figure 3. Since a single automation cycle takes approximately 105 minutes for a lab-scale reactor, considerably longer for container-scale systems, optimizing all possible channel concepts and selecting the most effective one becomes a time-intensive process. Therefore, to enhance efficiency, there is a need to extend the tool with a pre-selection mechanism that can narrow down viable channel geometries prior to full optimization.

Beyond the reactor geometry, the tool offers further flexibility. The catalyst is currently modeled as an idealized spherical particle, so other catalyst geometries require appropriate flow modeling in both the CFD model and the PFR calculation. Multiple catalyst channels are already supported, while catalyst zones with differing properties would require an exten-

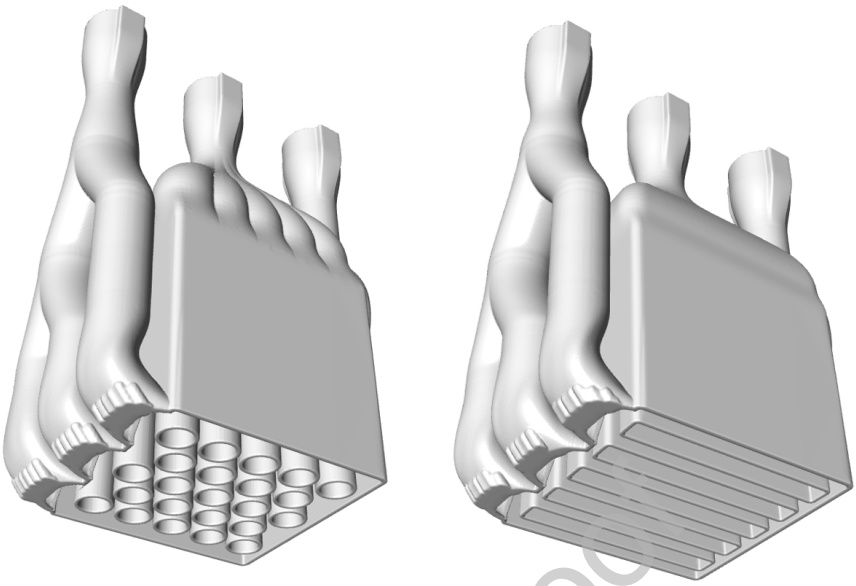

Figure 10: CAD renderings of two reactor designs with different internal channel geometries generated by the design automation tool: (i) circular and (ii) parallel rectangular channel configurations, demonstrating that different channel concepts can be produced without manual CAD remodeling

sion of the tool. Other reactor materials can be used by adjusting the material properties in the numerical simulations. In its current implementation, however, the tool is validated only for the employed kinetic model from [16] and for stainless steel 316L, and adaptation to other catalysts or alloys would require corresponding experimental validation.

6. Conclusion

This study presents a design automation tool to support the development of reactors for decentralized energy systems, with a particular focus on methanol synthesis. By integrating automated geometry generation, simulation-based performance evaluation, and AM constraints into a single workflow, the tool enables adaptable reactor design without the need for manual CAD modeling. The reliability of the generated designs is governed by the quality of the specified process conditions, hardware constraints, and reaction kinetics. The tool facilitates the development of reactors tailored to specific operational requirements, achieving a total design time of approximately 105 minutes for lab-scale reactors and 27 hours for container-scale systems. Our results indicate that optimizing both geometrical and process parameters using this automation tool leads to increased methanol production rates, especially for the large reactors. Experimental validation of the simulation results confirms that the tool can reliably generate functional lab-scale reactor designs, demonstrating its practical applicability and potential to support the transition to industrial-scale systems while addressing key upscaling challenges.

CRediT authorship contribution statement

Mertcan Kaya: Conceptualization, Data curation, Formal analysis, Investigation, Methodology, Software, Validation, Visualization, Writing – original draft.

Christoph Klahn: Conceptualization, Funding acquisition, Project administration, Supervision, Writing – review and editing.

All authors approved the final version of the manuscript and agree to be accountable for all aspects of the work, ensuring that questions related to the accuracy or integrity of any part of the work are appropriately investigated and resolved.

Data Availability

The data supporting the findings of this study are partially publicly available via GitHub at `https://github.com/mertcnkaya/PFR_MeOH`. The repository contains the implementation of the PFR optimization module, including the reaction kinetics and example input files, so that the initial reactor dimensioning can be reproduced. The Supplementary Material accompanying this article provides the analytical models underlying the PFR stage, the pressure-load calculation, further details of the CFD model, the calibration procedures, and the complete experimental dataset. Together, these sources allow the PFR stage to be reproduced and the reported experimental results, including the values underlying the statistical analyses and figures, to be recalculated. The FEA and CFD models are documented in sufficient detail to be reimplemented.

Certain components of the study, including parts of the reactor design tool and the associated computational framework, are not publicly available due to intellectual property considerations. The interfaces between the modules are nevertheless kept generic, since the parameters are exchanged between the PFR, FEA and CFD stages through a common CSV file and the generated geometry is transferred to the simulation environments in neutral CAD formats. Individual modules can therefore in principle be substituted without modifying the remaining workflow. These components may be made available in a limited form upon reasonable request to the corresponding author.

Declaration of generative AI and AI-assisted technologies in the writing process

During the preparation of this work the authors used ChatGPT in order to improve the readability and the language of the manuscript. After using this tool, the authors reviewed and edited the content as needed and take full responsibility for the content of the published article.

Acknowledgment

The authors would like to express their sincere gratitude to Sirui Ye, Etienne Martin, and Kagan Sendal for their valuable contributions to this project as thesis students or research assistants. Their dedication and effort are instrumental to the success of various stages of the work. The authors also thank Manuel Hofheinz for his support in the manufacturing and post-processing of the PBF-LB/M reactor designs, and Cornelia Schorle for conducting the leakage and pressure tests.

This work is supported by the BMWE 3D-Process project (project no. 03EN2065E). 3D-Process is financed by Federal Ministry for Economic Affairs and Climate Protection from Germany.

References

[1] P. Gabrielli, M. Gazzani, M. Mazzotti, The role of carbon capture and utilization, carbon capture and storage, and biomass to enable a net-zero-CO_2 emissions chemical industry, Industrial & Engineering Chemistry Research 59 (15) (2020) 7033–7045. doi:10.1021/acs.iecr.9b06579.

[2] M. A. H. El-Sayed, A. M. T. Ibrahem, M. A. A. El-Sayed, Powering the future: A comprehensive review of battery energy storage systems, Energies 16 (17) (2023) 6344. doi:10.3390/en16176344.

[3] M. Usman, M. Imran, M. Asif, Prospects of carbon capture, utilization and storage for mitigating climate change in developing economies, Environmental Science: Advances 2 (3) (2023) 246–260. doi:10.1039/D2VA00236A.

[4] R. Amal, J. Scott, K. R. Catchpole, Z. Li, Y. H. Ng, G. W. P. Adcock, N. S. Lewis, Opportunities and challenges for renewable Power-to-X, ACS Energy Letters 5 (11) (2020) 3618–3639. doi:10.1021/acsenergylett.0c02249.

[5] V. Dieterich, A. Buttler, A. Hanel, H. Spliethoff, S. Fendt, Power-to-Liquid via synthesis of Methanol, DME or Fischer–Tropsch-Fuels: a review, Energy & Environmental Science 13 (10) (2020) 3207–3252. doi:10.1039/D0EE01187H.

[6] S. Brynolf, M. Taljegard, M. Grahn, J. Hansson, Global production potential of green methanol based on variable renewable electricity, Energy & Environmental Science 17 (2024) 3503–3522. doi:10.1039/D3EE02951D.

[7] F. Samimi, N. Hamedi, M. R. Rahimpour, Green methanol production process from indirect CO_2 conversion: RWGS reactor versus RWGS membrane reactor, Journal of Environmental Chemical Engineering 7 (1) (2019) 102813. doi:10.1016/j.jece.2018.102813.

[8] F. Bisotti, M. Fedeli, M. Manenti, F. Manenti, S. Pierucci, Impact of kinetic models on methanol synthesis reactor predictions: In silico assessment and comparison with industrial data, Industrial & Engineering Chemistry Research 61 (4) (2022) 1444–1456. doi:10.1021/acs.iecr.1c04476.

[9] J. L. da Silva Jr., H. S. Santana, M. J. Hodapp, Numerical evaluation of methanol synthesis in catalytic wall-coated microreactors: scale-up and performance analysis of planar and monolithic designs, Frontiers in Chemical Engineering 6 (2024) 1440657. doi:10.3389/fceng.2024.1440657.

[10] M. V. Bram, J. Liniger, S. S. Majidabad, H. R. Shabani, M. P. R. Teles, X. Cui, Challenges in Power-to-X: A perspective of the configuration and control process for e-methanol production, International Journal of Hydrogen Energy (2024) 315–325doi:10.1016/j.ijhydene.2024.05.273.

[11] C. Parra-Cabrera, C. Achille, S. Kuhn, R. Ameloot, 3D printing in chemical engineering and catalytic technology: structured catalysts, mixers and reactors, Chemical Society Reviews 47 (1) (2018) 209–230. doi:10.1039/c7cs00631d.

[12] A. Hauser, M. Neubert, A. Feldner, A. Horn, F. Grimm, J. Karl, Design and implementation of an additively manufactured reactor concept for the catalytic methanation, Applied Sciences 12 (18) (2022) 9393. doi:10.3390/app12189393.

[13] B. Gutmann, M. Köckinger, G. Glotz, T. Ciaglia, E. Slama, M. Zadravec, S. Pfanner, M. C. Maier, H. Gruber-Wölfler, C. O. Kappe, Design and 3D printing of a stainless steel reactor for continuous difluoromethylations using fluoroform, Reaction Chemistry & Engineering 2 (6) (2017) 919–927. doi:10.1039/C7RE00176B.

[14] W. Hou, A. Bubliauskas, P. J. Kitson, J.-P. Francoia, H. Powell-Davies, J. M. P. Gutierrez, P. Frei, J. S. Manzano, L. Cronin, Automatic generation of 3D-printed reactionware for chemical synthesis digitization using chemscad, Organic Chemistry Frontiers 8 (5) (2021) 1060–1067. doi:10.1039/D0QO01154A.

[15] M. Kaya, C. Klahn, Design for additive manufacturing education of process engineering students on an industrial challenge, Procedia CIRP 128 (2024) 911–916, 34th CIRP Design Conference. doi:10.1016/j.procir.2024.06.044.

[16] B. L. de Oliveira Campos, K. H. Delgado, S. Wild, F. Studt, S. Pitter, J. Sauer, Surface reaction kinetics of the methanol synthesis and the water gas shift reaction on $Cu/ZnO/Al_2O_3$, Reaction Chemistry & Engineering 6 (5) (2021) 868–887. doi:10.1039/D1RE00040C.

[17] Y. Zhou, X. Li, J. Wang, H. Chen, Research on biomass energy and CO_2 conversion to methanol: a combination of conventional and bibliometric review analysis, Carbon Research 1 (1) (2024) 12–25. doi:10.1007/s44246-024-00179-0.

[18] M. Ebrahimzadeh Sarvestani, O. Norouzi, F. Di Maria, A. Dutta, From catalyst development to reactor design: A comprehensive review of methanol synthesis techniques, Energy Conversion and Management 302 (2024) 118070. doi:10.1016/j.enconman.2024.118070.

[19] L. Air Products Liquid Phase Conversion Co., Commercial-scale demonstration of the liquid phase methanol (LPMEOH™) process. final report, volume 2: Project performance and economics, Tech. Rep. DE-FC22-92PC90543, U.S. Department of Energy (June 2003).
URL `https://www.osti.gov/biblio/827411`

[20] S. Motahari, S. F. Moorjani, M. R. Rahimpour, Methanol production: A comprehensive review of processes, catalysts, and reactors, in: Reference Module in Chemistry, Molecular Sciences and Chemical Engineering, Elsevier, 2024, pp. 1–25. doi:10.1016/B978-0-443-15740-0.00067-7.

[21] H. Bakhtiary-Davijany, F. Hayer, X. Kim Phan, R. Myrstad, H. J. Venvik, P. Pfeifer, A. Holmen, Modelling and simulation of a single slit micro packed bed reactor for methanol synthesis, Catalysis Today 343 (2020) 226–233. doi:10.1016/j.cattod.2019.05.026.

[22] S. Arab, J.-M. Commenge, J.-F. Portha, L. Falk, Methanol synthesis from CO_2 and H_2 in multi-tubular fixed-bed reactor and multi-tubular reactor filled with monoliths, Chemical Engineering Research and Design 92 (11) (2014) 2598–2608. doi:10.1016/j.cherd.2014.03.009.

[23] D. Li, T. Maloney, N. Mannan, S. A. Niknam, Design of additively manufactured methanol conversion reactor for high throughput production, Material Design & Processing Communications 3 (1) (2020) e143. doi:10.1002/mdp2.143.

[24] M. L. Schulte, V. Truttmann, D. E. Doronkin, L. Baumgarten, A. Nicolai, D. A. Montalvo Beltran, F. J. Summ, C. Kiener, L. Warmuth, S. Pitter, E. Saraçi, J.-D. Grunwaldt, Monitoring the fate of zn in the cu/zno/zro2 catalyst during co2-to-methanol synthesis at high conversions by operando spectroscopy, Angewandte Chemie International Edition 64 (15) (2025). doi:10.1002/anie.202423281.

[25] D. F. Metzger, C. Klahn, R. Dittmeyer, Downsizing sustainable aviation fuel production with additive manufacturing—an experimental study on a 3D printed reactor for fischer-tropsch synthesis, Energies 16 (19) (2023) 6798. doi:10.3390/en16196798.

[26] I. Gibson, D. Rosen, B. Stucker, M. Khorasani, Additive Manufacturing Technologies: 3D Printing, Rapid Prototyping, and Direct Digital Manufacturing, 3rd Edition, Springer, Cham, Switzerland, 2021. doi:10.1007/978-3-030-56127-7.

[27] C. Klahn, B. Leutenecker-Twelsiek, Design guidelines, in: E. Pei, A. Bernard, D. Gu, C. Klahn, M. Monzón, M. Petersen, T. Sun (Eds.), Springer Handbook of Additive Manufacturing, Springer Handbooks, Springer International Publishing, Cham, 2023, Ch. 12, pp. 177–198. doi:10.1007/978-3-031-20752-5_12.

[28] D. Thomas, The development of design rules for selective laser melting, Ph.D. thesis, 2009 (University of Wales Institute). doi:10.25401/cardiffmet.20974597.v1.

[29] J. Kranz, Methodik und Richtlinien für die Konstruktion von laseradditiv gefertigten Leichtbaustrukturen, Springer Vieweg, Berlin, Heidelberg, 2017. doi:10.1007/978-3-662-55339-8.

[30] S. Safavi, M. Tarkian, Collaborative multidisciplinary design optimization: A framework applied on aircraft conceptual system design, Concurrent Engineering 23 (2) (2015) 99–110. doi:10.1177/1063293X15587020.

[31] S. Nambiar, A. A. Ananno, H. Titus, A. Wiberg, M. Tarkian, Multidisciplinary automation in design of turbine vane cooling channels, International Journal of Turbomachinery, Propulsion and Power 9 (1) (2024) 7. doi:10.3390/ijtpp9010007.

[32] K. Amadori, M. Tarkian, J. Ölvander, P. Krus, Flexible and robust CAD models for design automation, Advanced Engineering Informatics 26 (2) (2012) 180–195. doi:10.1016/j.aei.2012.01.004.

[33] A. Lindblad, J. Malm, C. Johansson, K. Shea, R. Söderberg, Design automation strategies for aerospace components during conceptual design phases, in: Aerospace Europe Conference 2023 – 10th EUCASS – 9th CEAS, 2023, pp. 99–104. doi:10.13009/EUCASS2023-578.

[34] M. Biedermann, M. Meboldt, Computational design synthesis of additive manufactured multi-flow nozzles, Additive Manufacturing 35 (2020) 101231. doi:10.1016/j.addma.2020.101231.

[35] M. Stokes, Managing Engineering Knowledge: MOKA Methodology for Knowledge Based Engineering Applications, Professional Engineering Publishing, London, 2001.

[36] B. Leischer, Methodisches Konstruieren in Ausbildung und Beruf: Praxisorientierte Konstruktionsentwicklung und Rechnergestützte Optimierung, Springer Fachmedien Wiesbaden, 2019. doi:10.1007/978-3-658-26042-0.

[37] H. Li, R. Lachmayer, Automated exploration of design solution space applying the generative design approach, in: Proceedings of the Design Society: International Conference on Engineering Design, Vol. 1, 2019, pp. 1085–1094. doi:10.1017/dsi.2019.114.

[38] J. Cagan, C. M. McKown, Computational design synthesis: Model and applications, AI EDAM 19 (3) (2005) 182–198. doi:10.1017/S0890060405050130.

[39] G. Colombo, D. Pugliese, P. Klein, A study for neutral format to exchange and reuse engineering knowledge in KBE applications, in: International Conference on Engineering, Technology and Innovation: Engineering Responsible Innovation in Products and Services, 2014, pp. 99–104. doi:10.1109/ICE.2014.6871565.

[40] T. Savage, N. Basha, J. McDonough, J. Krassowski, O. K. Matar, E. A. del Rio Chanona, Machine learning-assisted discovery of flow reactor designs, Nature Chemical Engineering (2023). doi:10.1038/s44286-024-00099-1.

[41] M. Biedermann, P. Beutler, M. Meboldt, Routing multiple flow channels for additive manufactured parts using iterative cable simulation, Additive Manufacturing 56 (2022) 102891. doi:10.1016/j.addma.2022.102891.

[42] M. Kaya, J. Ferchow, M. Meboldt, C. Klahn, Machine learning-assisted design automation workflow of non-uniform flow distributors for multipass crossflow device, Results in Engineering 27 (2025) 106931. doi:10.1016/j.rineng.2025.106931.

[43] M. Seifrid, A. Aspuru-Guzik, You wouldn't download a molecule! now, chemscad makes it possible, ACS Central Science 7 (2) (2021) 228–230. doi:10.1021/acscentsci.1c00108.

[44] M. Kaya, C. Klahn, Sequential parameter optimization for algorithm-based design generation using data from multiphysics simulations, Procedia CIRP 119 (2023) 1234–1239, the 33rd CIRP Design Conference. doi:10.1016/j.procir.2023.02.191.

[45] M. Son, Y. Woo, G. Kwak, Y.-J. Lee, M.-J. Park, Cfd modeling of a compact reactor for methanol synthesis: Maximizing productivity with increased thermal controllability, International Journal of Heat and Mass Transfer 145 (2019) 118776. doi:10.1016/j.ijheatmasstransfer.2019.118776.

[46] M. R. Rahimpour, M. Lotfinejad, Enhancement of methanol production in a membrane dual-type reactor, Chemical Engineering & Technology 30 (8) (2007) 1062–1076. doi:10.1002/ceat.200700114.

[47] F. Nestler, A. Schütze, M. Ouda, M. Hadrich, A. Schaadt, S. Bajohr, T. Kolb, Kinetic modelling of methanol synthesis over commercial catalysts: A critical assessment, Chemical Engineering Journal 394 (2020) 124881. doi:10.1016/j.cej.2020.124881.

[48] C. Seidel, A. Jörke, B. Vollbrecht, A. Seidel-Morgenstern, A. Kienle, Kinetic modeling of methanol synthesis from renewable resources, Chemical Engineering Science 175 (2018) 130–138. doi:10.1016/j.ces.2017.09.043.

[49] D. Khatamsaz, B. Vela, P. Singh, D. D. Johnson, D. Allaire, R. Arróyave, Bayesian optimization with active learning of design constraints using an entropy-based approach, npj Computational Materials 9 (2023) 49. doi:10.1038/s41524-023-01006-7.

[50] J. A. Paulson, C. Tsay, Bayesian optimization as a flexible and efficient design framework for sustainable process systems, Current Opinion in Green and Sustainable Chemistry 51 (2025) 100983. doi:10.1016/j.cogsc.2024.100983.

[51] M. Kaya, PFR_MeOH: Plug flow reactor model for methanol synthesis, `https://github.com/mertcnkaya/PFR_MeOH`, gitHub repository (2025).

[52] F. Li, R. Patton, K. Moghal, The relationship between weight reduction and force distribution for thin wall structures, Thin-Walled Structures 43 (4) (2005) 591–616. doi:10.1016/j.tws.2004.10.006.

[53] A. Alonzo-García, C. del Carmen Gutiérrez-Torres, J. A. Jiménez-Bernal, Computational fluid dynamics in turbulent flow applications, in: R. Lopez-Ruiz (Ed.), Numerical Simulation, IntechOpen, Rijeka, 2016, Ch. 13, pp. 315–336. doi:10.5772/63831.

[54] Directive 2014/68/eu of the european parliament and of the council of 15 may 2014 on the harmonisation of the laws of the member states relating to the making available on the market of pressure equipment, `https://eur-lex.europa.eu/legal-content/EN/TXT/?uri=CELEX:32014L0068`, official Journal of the European Union, L 189/164, 27.6.2014 (2014).

[55] F. Grinschek, A. Charles, A. Elkaseer, C. Klahn, S. G. Scholz, R. Dittmeyer, Gas-tight means zero defects - design considerations for thin-walled fluidic devices

with overhangs by laser powder bed fusion, Materials & Design 223 (2022) 111174. doi:10.1016/j.matdes.2022.111174.

[56] H. Rottländer, W. Umrath, G. Voss, Fundamentals of leak detection, Leybold GMBH (ed) Cat 199 (2016) 37.

[57] J. M. Bonem, Potential Problems With Scale-up, in: J. M. Bonem (Ed.), Chemical Projects Scale Up, Elsevier, 2018, pp. 1–15. doi:10.1016/B978-0-12-813610-2.00001-5.

[58] G. H. Graaf, E. J. Stamhuis, A. A. C. M. Beenackers, Kinetics of low-pressure methanol synthesis, Chemical Engineering Science 43 (12) (1988) 3185–3195. doi:10.1016/0009-2509(88)85127-3.

Declaration of interests

Mertcan Kaya reports financial support was provided by Federal Ministry for Economic Affairs and Energy. If there are other authors, they declare that they have no known competing financial interests or personal relationships that could have appeared to influence the work reported in this paper.